



HAL
open science

Processes controlling the seasonal cycle of wave-dominated inlets

X. Bertin, André Fortunato, Guillaume Dodet

► **To cite this version:**

X. Bertin, André Fortunato, Guillaume Dodet. Processes controlling the seasonal cycle of wave-dominated inlets. *Journal of Integrated Coastal Zone Management*, 2015. ⟨hal-03676631⟩

HAL Id: hal-03676631

<https://hal.science/hal-03676631v1>

Submitted on 24 May 2022

HAL is a multi-disciplinary open access archive for the deposit and dissemination of scientific research documents, whether they are published or not. The documents may come from teaching and research institutions in France or abroad, or from public or private research centers.

L'archive ouverte pluridisciplinaire HAL, est destinée au dépôt et à la diffusion de documents scientifiques de niveau recherche, publiés ou non, émanant des établissements d'enseignement et de recherche français ou étrangers, des laboratoires publics ou privés.



HAL Authorization

Processes controlling the seasonal cycle of wave-dominated inlets

Processos que controlam o ciclo sazonal de embocaduras dominadas pelas ondas

Xavier Bertin,¹ André Fortunato² and Guillaume Dodet^{1,2}

¹UMR 7266 LIENSs, CNRS-La Rochelle University, 2 rue Olympe de Gouges, 17000 La Rochelle, France. xbertin@univ-lr.fr, gdodet01@univ-lr.fr

²Laboratório Nacional de Engenharia Civil, Avenida do Brasil, 101, Lisboa, Portugal. afortunato@lnec.pt

Abstract

This paper reviews the physical processes controlling wave-dominated inlets, based on several studies conducted at two inlets located on the West Coast of Portugal. Once the observed hydrodynamics and morphological changes are reasonably simulated, numerical experiments are performed to explain the development of the inlet during fair weather conditions and its shoaling and closure during winter storms. The former behaviour is explained by a tidal distortion that promotes ebb-dominance while the latter is explained by the combination of several wave-related processes: (1) the “bulldozer effect” due to the shore-normal component of wave forces; (2) the presence of lateral barotropic pressure gradients, accelerating longshore flows towards the inlet; (3) wave blocking during the ebb and (4) a rise in mean sea level, peaking in late autumn. Recent results also suggest that infragravity waves may play a major role.

Key words: Tidal inlets, wave-induced processes, wave blocking, infragravity, Óbidos lagoon, Albufeira lagoon.

Resumo

Apresenta-se uma revisão dos processos físicos que controlam a dinâmica de embocaduras dominadas pelas ondas, com base em vários estudos conduzidos em duas embocaduras localizadas na zona costeira centro de Portugal. As análises são conduzidas com modelos morfodinâmicos, que reproduzem adequadamente a hidrodinâmica e a evolução morfológica observadas. Experiências numéricas são efetuadas para explicar o desenvolvimento das embocaduras durante o verão marítimo e a sua colmatção e fecho durante tempestades de inverno. O primeiro comportamento é explicado pela distorção da maré que promove a dominância da vazante, enquanto o segundo se explica pela combinação de vários processos relacionados com a agitação marítima: (1) o “efeito bulldozer” devido à componente transversal à costa das forças devidas às ondas; (2) a presença de gradientes laterais de pressão barotrópica, que aceleram as correntes longitudinais em direcção à embocadura; (3) o bloqueamento das ondas durante a vazante e (4) o ciclo sazonal do nível médio do mar, cujo pico ocorre no outono. Resultados recentes sugerem ainda que as ondas infragravíticas podem ter um papel importante nesta dinâmica.

Palavras-chave: embocaduras de maré, processos induzidos pelas ondas, bloqueamento das ondas, ondas infragravíticas, lagoa de Óbidos, Lagoa de Albufeira.

1. Introduction

The economic and environmental importance of tidal inlets has been growing worldwide, while their sustainable management faces many conflicting challenges, such as the maintenance of open navigation routes, the stability of the adjacent shoreline or the water renewal in the back-barrier lagoons. The combined action of waves and tides and the presence of shallow channels often drive a fast and intense sediment dynamics and make their behaviour difficult to predict. These problems are particularly relevant at wave-dominated inlets, where this intense dynamics can drive fast and large morphological changes within a few days/weeks. Eventually, wave-dominated inlets can episodically or seasonally close, although the responsible physical processes remain only partly understood.

To improve the understanding of tidal inlet dynamics, a promising avenue is the development and application of morphodynamic modelling systems. These modelling systems consist of a set of modules to simulate tidal hydrodynamics, wave propagation, sediment transport and bottom evolution.

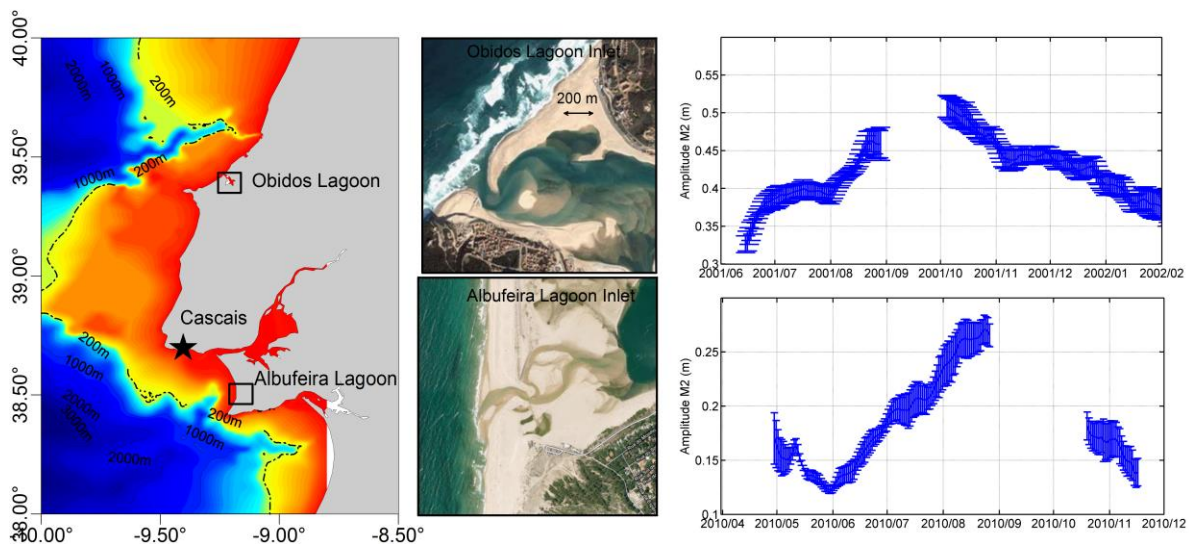
58 The morphodynamic modelling of tidal inlets already met several successes over the last decade
 59 (Cayocca, 2001; Dastgheib et al., 2008; Bertin et al., 2009a; Bruneau et al., 2011). Nevertheless, to
 60 date, the successful simulation of tidal inlet closure is restricted to simplified/empirical approaches
 61 (Ranasinghe et al., 1999) and/or synthetic tidal inlets (Walstra et al. 2009). This problem suggests that
 62 the dominant physical processes are not all captured by most modelling systems. However, the
 63 numerical modelling of wave-dominated inlets made significant progresses over the last decade, and
 64 resulted namely in an improved understanding of the main physical processes that drive morphological
 65 changes.

66 This paper reviews the knowledge gained from previous modelling-based studies performed at two
 67 wave-dominated inlets located on the west coast of Portugal (Bertin et al., 2009b; Bruneau et al., 2011;
 68 Dodet et al., 2013; Fortunato et al., 2014) and synthesizes the physical processes controlling the
 69 seasonal cycle of wave-dominated inlets, including their enlargement during fair weather conditions
 70 and their shoaling or even closure during winter months.

71
 72 **2. Study sites**

73
 74 This study is based on results obtained at two wave-dominated inlets located on the West Coast of
 75 Portugal: the Albufeira Lagoon Inlet and the Óbidos Lagoon Inlet (figure 1). Tides are semi-diurnal
 76 and range from 0.5 m to 3.5 m (meso-tidal). When tides propagate into the lagoons, the semi-diurnal
 77 tidal constituents are severely damped, with the amplitude of M2 typically decreasing by 50 to 80 %
 78 (figure 1) at both lagoons (Oliveira et al., 2006; Bertin et al., 2009b; Dodet et al., 2013). Tidal
 79 amplitude in the lagoon experiences a seasonal cycle, with a maximum at the end of the summer and a
 80 minimum at the end of the winter at Óbidos. In the Albufeira Lagoon Inlet usually closes in autumn
 81 (figure 1). In contrast to semi-diurnal constituents, quarter-diurnal and fortnightly non-linear tidal
 82 constituents develop inside the lagoons, resulting in a strongly distorted tidal signal, with ebb lasting 7
 83 to 8 hours and floods 4.5 to 5.5 hours. Freshwater discharges are usually negligible compared to the
 84 dynamics induced by waves and tides, particularly in Albufeira where the lagoon is closed from
 85 autumn to mid-spring.

86



87
 88 Figure 1. Bathymetric map of the central western coast of Portugal, aerial view of the Albufeira and Óbidos lagoon inlets and
 89 time-series of the amplitude of the constituent M2 inside those lagoons based on water level measurements.

90
 91 Figura 1. Batimetria da zona centro da costa Portuguesa, vista aérea das embocaduras das lagoas de Óbidos e Albufeira e
 92 séries temporais da amplitude da constituinte M2 nestas lagoas, baseadas em medições de altura de água.

93 The continental shelf in front of both inlets is very narrow (< 20 km), which causes these inlets to
 94 be exposed to a very energetic wave climate, particularly in winter. Based on a 57-year wave
 95 numerical hindcast (Dodet et al., 2010), the mean annual deep water (10.0°W ; 38.0°N ; ~ 3000 m deep)
 96 significant wave height (H_s), mean direction (MWD) and peak period (T_p) are respectively 1.9 m, 312
 97 $^{\circ}$, and 10.5 s. During winter (resp. summer) the corresponding values are: 2.5 m, 305° , and 12.1 s

98 (resp. 1.3 m, 319 ° and 8.4 s). Also, the presence of coarse sediments (i.e. d50 in the range 0.5-1.0 mm)
99 causes the adjacent beaches to display steep faces, which favour energetic wave breaking and large
100 sediment transport rates. This severe wave climate combined to the meso-tidal range and shallow
101 channels leads to very dynamic inlets, with channel migration which can reach 50 m.week⁻¹(Fortunato
102 et al., 2014). Both systems are characterized by a seasonal cycle, with an enlargement and deepening
103 of the main channel during the summer period and a strong shoaling during the winter period (Bertin
104 et al., 2009b; Fortunato et al., 2014).

105 **3. Data and methods**

106 **2.1. Field measurements**

107
108
109
110 At both sites, several field campaigns were carried out over the last decade, where pressure sensors,
111 electromagnetic current-meters and ADCPs were deployed over both the flood and the ebb deltas, in
112 order to characterize wave and tide transformation along their propagation through the inlets. Pressure
113 sensors were also deployed during several months inside the lagoons in order to characterize properly
114 the seasonal evolution of tidal amplitude. Finally, repetitive bathymetric and topographic surveys were
115 carried out to quantify the fast morphological changes observed at both sites. Details on these field
116 measurements and data processing can be found in Oliveira et al. (2006), Bertin et al. (2009b), Dodet
117 et al. (2013) and Fortunato et al. (2014).

118 **2.2. Numerical modelling system**

119
120
121 The numerical results presented in this study rely on the unstructured-grid modelling systems
122 MORSYS2D (Fortunato and Oliveira, 2004; Bertin et al., 2009b) and SELFE (Dodet et al., 2013;
123 Roland et al. 2012). These modelling systems share the same philosophy and fully couple a spectral
124 wave model (either SWAN, Boijj et al., 1999; or WWMII, Roland et al., 2012), a 2DH circulation
125 model (either ELCIRC, Zhang et al., 2004; or SELFE, Zhang et al; 2011) and a sediment
126 transport/bottom update model (either SAND2D, Fortunato and Oliveira, 2004; Bertin et al., 2009b; or
127 SED2D, Dodet, 2103). For both sites, the unstructured grids have a spatial resolution ranging from
128 about 500 m along the open boundary to 5 m along the coast in order to adequately represent the surf
129 zone and wave-induced flows. The numerical procedure can be seen on figure 2 and includes three
130 main steps:

131
132 1-First, the propagation of short waves is simulated using a spectral wave model forced along its
133 open boundary by time-series of spectra originating from the regional wave model of Dodet et al.
134 (2010). The spectral wave model is fed by fields of elevation and currents originating from the
135 circulation model.

136
137 2-The horizontal circulation is simulated using SELFE or ELCIRC, which is forced along its open
138 boundary by the 16 main tidal constituents whose amplitude and phase are computed with the regional
139 tidal model of Bertin et al. (2012). A full coupling is achieved with the spectral wave model through
140 gradients of radiation stresses, horizontal viscosity and bottom friction.

141
142 3-Sand fluxes are computed based on time-series of currents, water levels and wave parameters by
143 means of total transport empirical formulae (e.g. Soulsby and Van Rijn, Soulsby, 1997). The Exner or
144 sediment continuity equation is then solved using a node-centred finite volume method.
145
146

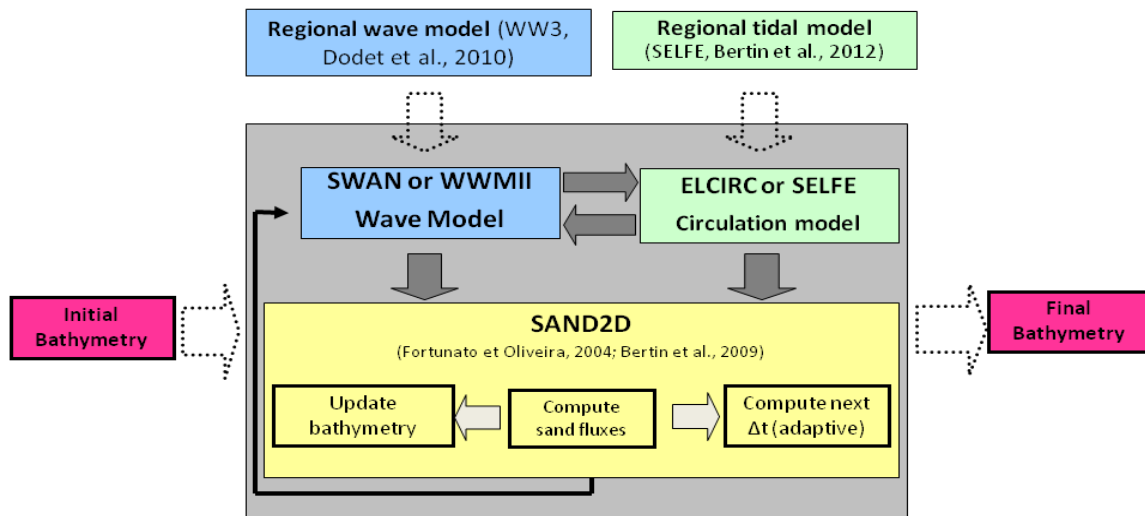


Figure 2. Flowchart of the modelling system procedure.

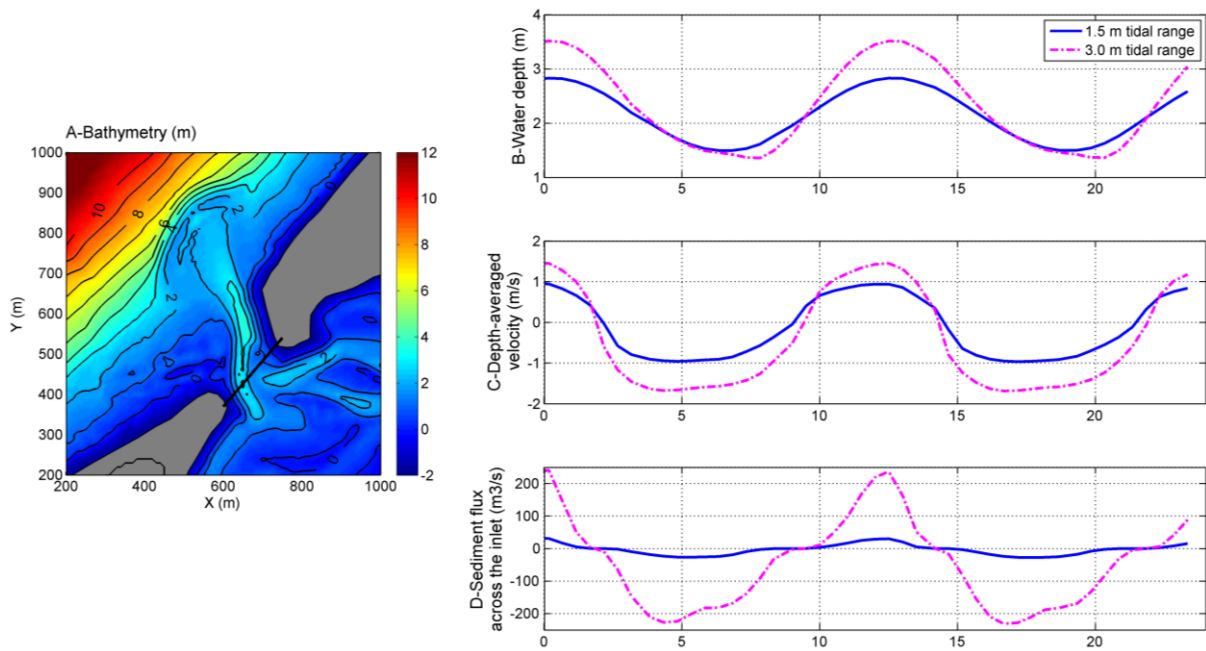
Figura 2. Esquema do modelo morfodinâmico.

4. Results and discussion

Previous studies conducted by our team have demonstrated that our modelling system was capable to reproduce waves and currents at the studied sites with a normalized root mean square error (hereafter NRMSE) of the order of 10-15 %. Water levels are predicted more accurately, with a NRMSE of the order of 5 % (Bertin et al., 2009b; Bruneau et al., 2011; Dodet et al., 2013). Morphological predictions have larger errors and their accuracy deteriorates with time along the simulation, although the main patterns are reproduced qualitatively. In particular, the enlargement of the main channel during fair weather conditions and its shoaling during winter months are well captured (Bertin et al., 2009a; Bruneau et al., 2011). In some cases, the model can also reproduce the meandering of the channels (Bruneau et al., 2011) and the inlet migration (Bertin et al, 2009c). Under these conditions, the dominant physical processes responsible for these morphological changes are assumed to be well captured by our modelling system. In this section, we present the results of numerical experiments that aim at describing and quantifying these processes.

4.1. Inlet development during fair weather conditions

In order to understand why wave-dominated inlets enlarge during fair weather conditions, we performed synthetic simulations at the Óbidos lagoon under tidal forcing only. We considered simplified tides represented by M2 only, whose amplitude was set to 0.75 m (mean neap conditions) and 1.5 m (mean spring conditions). Time series of water depth at the inlet reveal firstly that tides are strongly distorted at the inlet, with a shorter flood than ebb. This distortion is stronger for spring tides with an ebb duration of 7.5 h and a flood duration of 5.0 h. According to classical theories on tidal distortion for estuaries (e.g. Friedrichs and Aubrey, 1988), longer ebb would result in higher current velocities during flood. Yet, the opposite behaviour is observed at both inlets, with slightly larger velocities occurring during the ebb and lasting more than maximum flood velocities (figure 3-C). This paradoxical behaviour is related to the fact that maximum flood occurs for a water depth twice as large as maximum ebb, which causes ebb currents to be stronger so that mass conservation is ensured. Higher velocities in shallower depth during ebb cause associated sand fluxes to be 1.4 to 2.0 times larger than on flood (figure 3-D). As a consequence, under tidal forcing only, the Óbidos and Albufeira Lagoon inlets remain strongly ebb-dominated from velocity and sediment transport viewpoints, with a stronger ebb-dominance for spring tides compared to neap tides. This ebb-dominance favours the flushing of sediments at the inlet mouth and explains why wave-dominated inlets enlarge during fair weather conditions, when wave-related processes are not dominant.



187

188

189 Figure 3. (A) Bathymetry of the Óbidos Lagoon Inlet in July 2001 showing the profile where model outputs were averaged,
 190 (B) mean water depth across the inlet, (C) mean depth-averaged velocity across the inlet and (D) sediment fluxes integrated
 191 across the inlet.

192 **Figura 3. (A) Batimetria da embocadura da lagoa de Óbidos em julho de 2001, mostrando o perfil onde os**
 193 **resultados do modelo foram integrados, (B) profundidade média na embocadura, (C) média das**
 194 **velocidades médias na vertical e (D) fluxos sedimentares integrados através da embocadura.**

195

196 4.2. Inlet shoaling during winter period

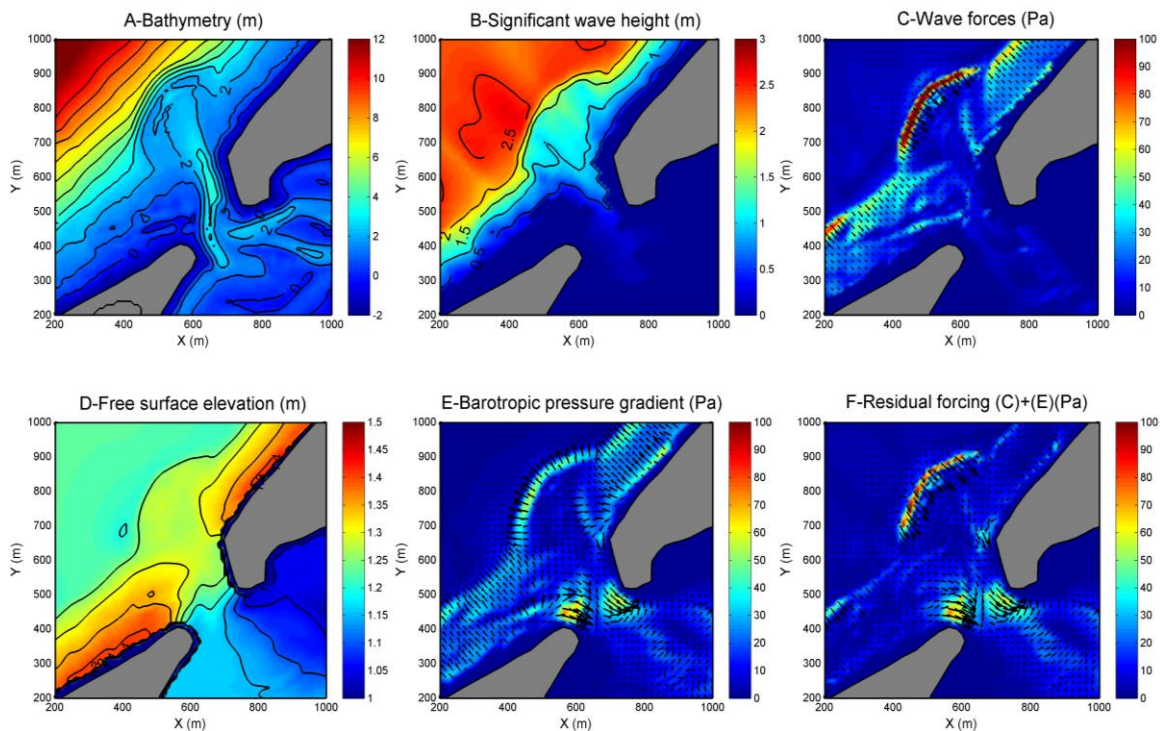
197

198 4.2.1. The “bulldozer effect”

199

200 Field observations revealed that wave-dominated inlets in Portugal experience shoaling during
 201 winter storms, occasionally leading to their closure (Bertin et al., 2009b; Fortunato et al., 2014). In
 202 order to understand which wave-related processes can induce the shoaling of wave-dominated inlets
 203 during winter storms, we performed a synthetic simulation at the Óbidos Lagoon considering energetic
 204 ($H_s = 3.0$ m; $T_p = 12$ s) shore-normal wave conditions with a 1.1 m tidal amplitude (mean annual tidal
 205 range). Figure 4-B shows that wave dissipation over the ebb-delta and at adjacent beaches results in
 206 large gradients of radiation stress (wave forces) directed onshore (figure 4-C). These forces induce a
 207 setup reaching 0.25 m at adjacent beaches, which itself induces a barotropic pressure gradient. At
 208 adjacent beaches, this barotropic pressure gradient nearly balances wave forces (figure 4-F) and the
 209 residual forces are very weak. In front of the inlet, large wave forces on the ebb delta are no longer
 210 balanced by a barotropic pressure gradient because the wave-induced setup is spread within the lagoon.
 211 As a result, a strong residual forcing occurs on the ebb delta, which was referred to as “bulldozer
 212 effect” by Hageman (1969). This phenomenon is well captured by our modelling system, which is able
 213 to reproduce the migration of ebb-delta sandbars towards the lagoon (Bertin et al., 2009b).

214



215
216
217 Figure 4. (A) Bathymetry (m), (B) significant wave height (m), (C) wave forces (Pa), (D) free surface elevation (m), (E)
218 barotropic pressure gradient (Pa) and (F) resultant forces (Pa) at the Óbidos Inlet for shore-normal offshore waves of $H_s = 3.0$
219 m.

220 Figura 4. (A) Batimetria (m), (B) altura significativa (m), (C) forças devidas às ondas (Pa), (D) elevação da
221 superfície livre (m), (E) gradiente de pressão barotrópica (Pa) e (F) resultante das forças (Pa) na embocadura da
222 Lagoa de Óbidos para ondas incidentes perpendiculares à costa com $H_s = 3.0$ m.

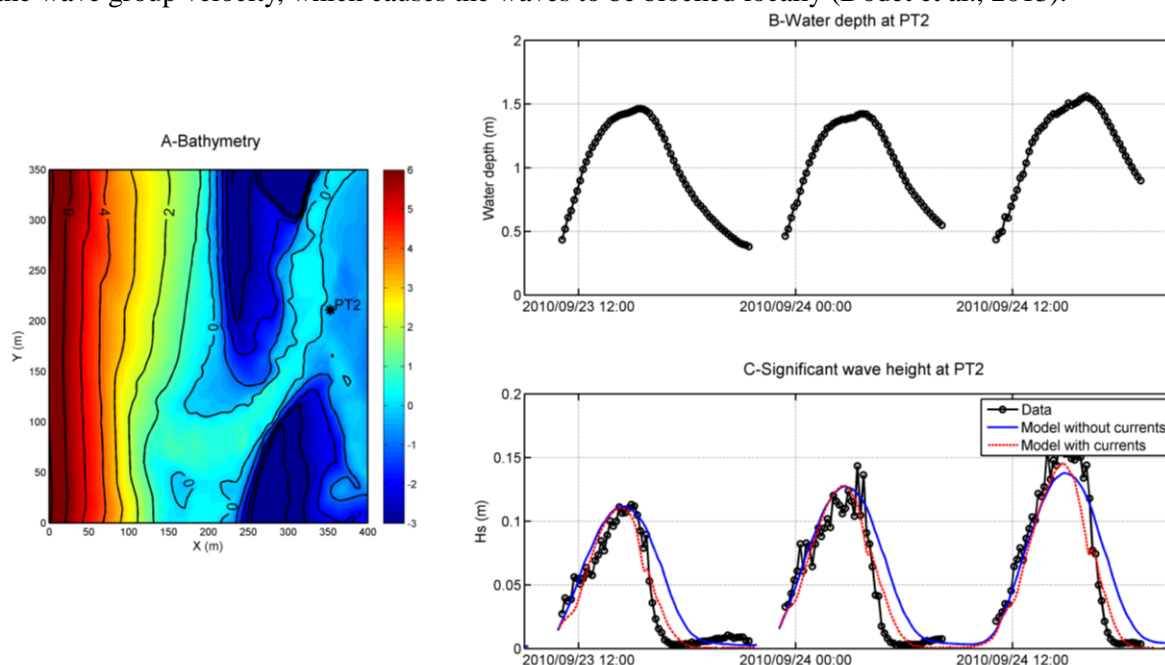
223
224 4.2.2. *Lateral barotropic pressure gradients*
225

226 Figure 4-D shows that wave forces induce a setup at adjacent beaches of the order of 10 % the
227 wave height at the breaking point. At the inlet, this setup is interrupted, which induces a lateral
228 barotropic pressure gradient. This barotropic pressure gradient is not compensated by any wave forces
229 so that a strong residual forcing directed towards the lagoon occurs on both sides of the inlet. These
230 pressure forces result in an acceleration of longshore currents towards the lagoon, which tend to push
231 large quantities of sediments into the lagoon. At high tide, this phenomenon is further enhanced by
232 wave refraction over the ebb-delta, which causes wave-induced longshore currents to converge
233 towards the inlet (not shown, Bertin et al., 2009b).

234
235 4.2.3. *Wave blocking during ebb*
236

237 A field campaign was carried out at the Albufeira Lagoon Inlet in September 2010 where
238 pressure transducers were deployed on both the ebb and the flood deltas (figure 5-A). A time series of
239 significant wave heights on the flood delta (PT2, figure 5-B) revealed firstly that the wave height
240 inside the lagoon is modulated along the tidal cycle and becomes almost nil at low tide. This behaviour
241 is due to wave energy dissipation by breaking on the ebb delta, which increases as water level
242 decreases. Furthermore, H_s are not symmetrical for a given water level and experience a fast drop
243 when ebb currents start to establish. To better understand this behaviour, the modelling system was run
244 with and without current feedback on wave propagation. Figure 5-B shows that the fast drop in H_s is
245 only reproduced if the feedback of currents in the wave model is taken into account. The modelling
246 results show firstly that waves propagating against currents experience whitecapping dissipation
247 (Dodet et al., 2013). This process is represented in our modelling system following the approach of

248 Westhuysen (2012). Two hours after the beginning of the ebb, wave heights inside the lagoon become
 249 almost nil. The analysis of modelled tidal currents reveals that, in the inlet main channel, waves
 250 propagate against tidal currents locally exceeding 2.0 m/s. Such large velocities almost correspond to
 251 the wave group velocity, which causes the waves to be blocked locally (Dodet et al., 2013).



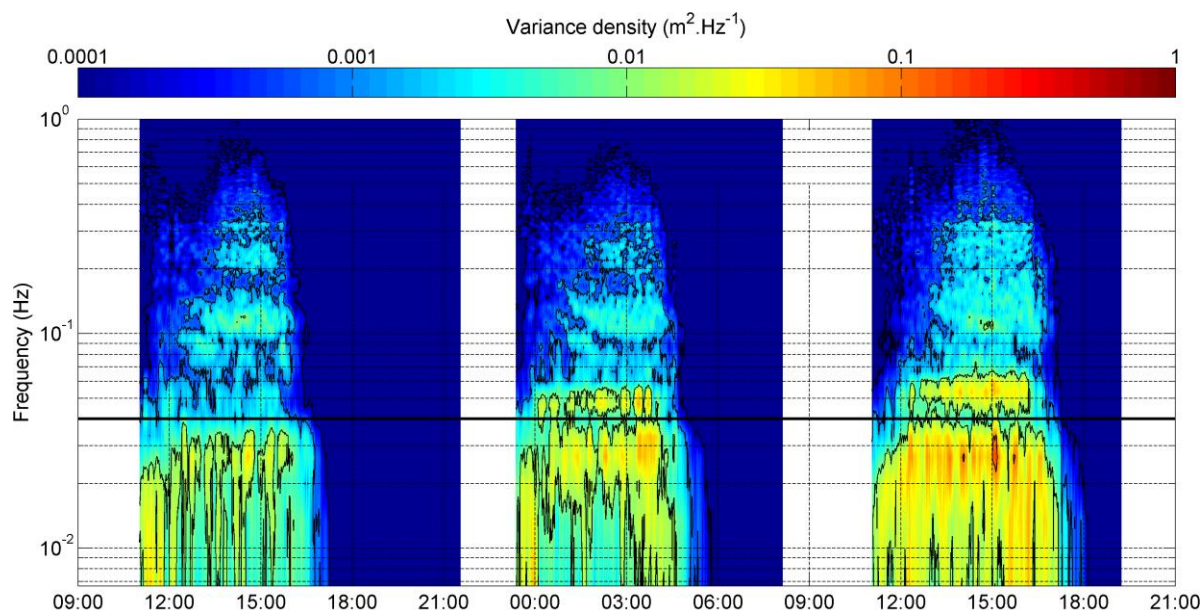
252 Figure 5. (A) Bathymetry of the Albufeira Lagoon Inlet, (B) measured water depth and (C) measured and
 253 modelled time series of significant wave heights on the flood delta in September 2010.
 254
 255 Figura 5. (A) Batimetria da emocadura da Lagoa de Albufeira, (B) altura de água medida e (C) séries temporais,
 256 medidas e simuladas, da altura significativa no banco de enchente em setembro de 2010.

257
 258 Dodet et al. (2013) investigated the impact of these phenomena on the sediment dynamics of tidal
 259 inlets. On flood, the presence of waves superimposed on tidal currents in the main channel increases
 260 sediment transport rates. During the ebb, waves are first dissipated by whitecapping, and then blocked,
 261 so that the transport capacity of ebb currents is no longer enhanced. Over a tidal cycle, these processes
 262 decrease the capacity of the inlet to flush sediments out of the lagoon. Nevertheless, further research is
 263 needed to determine whether this conclusion can be extended to other wave conditions and inlet
 264 configurations. Further experiments will have to be carried out during more energetic wave conditions
 265 and/or at wider inlets, where larger waves can propagate in the main channel.

266 4.2.4. Infragravity waves

267
 268
 269 A spectral analysis of pressure transducer and current data collected at the Albufeira Lagoon
 270 Inlet in September 2010 (figure 5-A) showed that a significant part of spectral energy was found in the
 271 infragravity band (0.004 Hz - 0.04 Hz, figure 6). This phenomenon is particularly clear on the third
 272 tidal cycle, where more energy is found on the infra-gravity band than the gravity band (figure 6). This
 273 low-frequency energy is expressed as low-frequency fluctuations of the free-surface elevation, wave
 274 heights and current velocities. These fluctuations were particularly visible in the measured data at PT2,
 275 when comparing the 1-min running averaged with the 60-min running averaged time-series (figure 7).
 276 Such oscillations reached up to 10 %, 20 % and 50 % of the 60-min filtered signal, for free-surface
 277 elevation, wave heights and currents, respectively. While the physical processes that explain these
 278 infragravity fluctuations require further investigation, Dodet (2013) estimated their contribution to the
 279 sediment dynamics of the inlet – aside from the effect of wave-current interactions. In this context, the
 280 total transport induced by waves and currents was computed at PT2 (figure 5A), using the Soulsby and
 281 Van Rijn formula (Soulsby, 1997), fed on the one hand by the 60-min filtered time-series of elevation,

282 H_s and velocity (the wave orbital velocity was computed using the linear theory) and on the other hand
 283 the 1-min filtered time-series that include the low-frequency oscillations. During the third tidal cycle,
 284 where low frequency fluctuations were the largest, the total sediment transport was locally up to eight



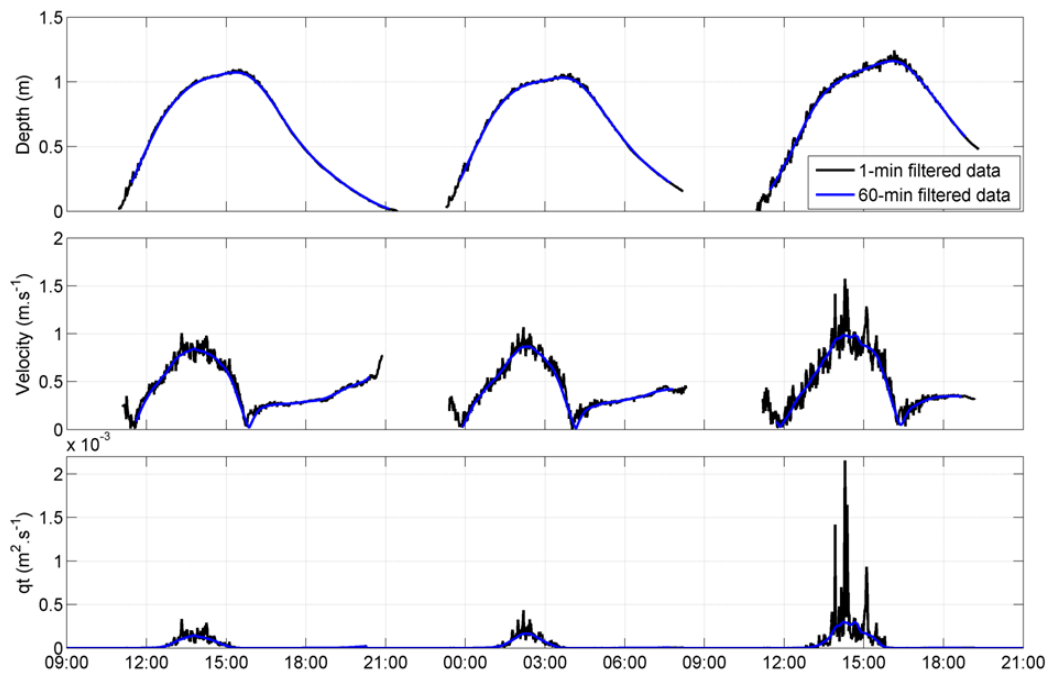
285 times as large when taking into account low-frequency fluctuations and twice as large when integrated
 286 over a tidal cycle.

287
 288 Figure 6. Energy spectra of the free surface elevation at PT2 (figure 5A), showing that a large part of the energy
 289 is located in the infragravity band.

290 **Figura 6. Espectro de energia da superfície livre na estação PT2 (Figura 5A), mostrando que grante parte**
 291 **da energia está localizada na banda infragravítica.**

292
 293 It can also be noted that these low-frequency fluctuations appear mostly during the flood,
 294 which suggests that infragravity waves are also damped or blocked by ebb currents. Therefore, in
 295 terms of inlet morphodynamics, this behaviour implies that these low-frequency fluctuations rather
 296 contribute to fill the lagoon with sediments. This process can play a key role during storms, where it
 297 can significantly contribute to inlet closure. However, according to the authors' knowledge, it is the
 298 first time that the importance of infragravity waves at tidal inlets is demonstrated and thus further
 299 research is needed. Namely, comparisons at other sites are required and the implementation of
 300 infragravity waves in modelling systems (e.g. Roelvink, 2009) would be a promising perspective.

301



302
303
304
305
306
307
308

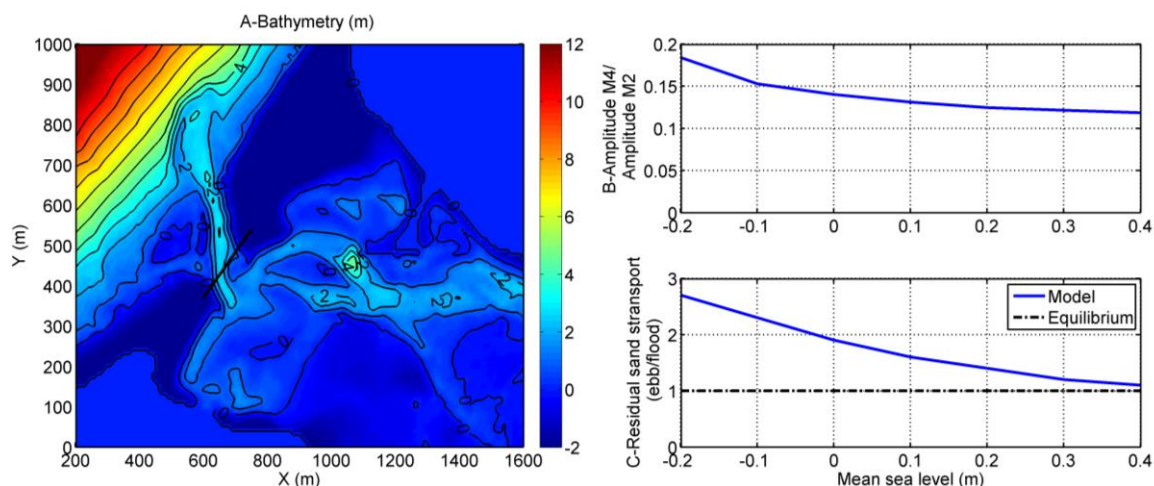
Figure 7. 1-min and 60-min running averaged time-series of water depth, velocity, and total sediment transport (Qt) at PT2 (figure 5).

Figura 7. Médias de banda móvel de 1 e 60 minutos da altura de água, velocidade e fluxo sedimentar total (Qt) em PT2 (Figura 5).

309 4.2.5. Variations in mean-sea level

310
311
312
313
314
315
316
317
318
319
320
321
322

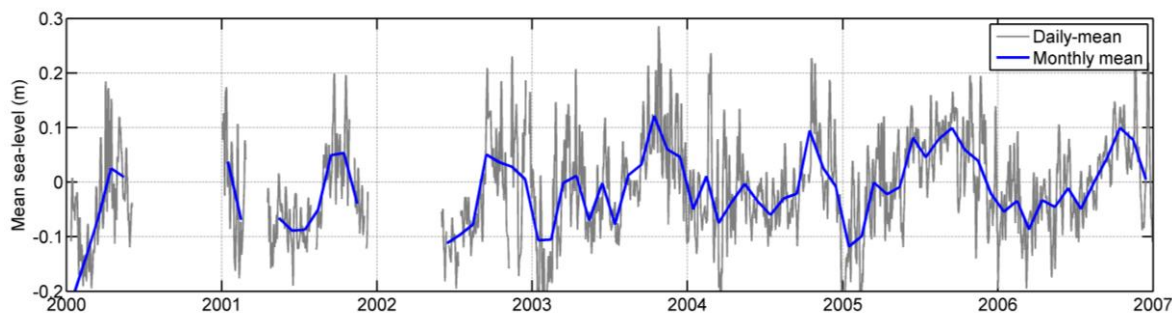
Previous studies have shown that at both Óbidos (Bertin et al., 2009b) and Albufeira (Dodet et al., 2013), the setup induced by wave breaking in front of the inlet propagates inside the lagoon and reaches roughly 10 % of the wave height at breaking. Energetic waves and winter storms can thus induce variations of mean sea-level (hereafter MSL) of a few tens of centimetres. Since both inlets are very shallow, such variations in MSL are expected to impact tidal asymmetry and thereby sediment dynamics significantly. To better quantify this phenomenon, morphodynamic simulations were performed at the Óbidos inlet under tidal forcing only and varying MSL between -0.2 m and +0.4 m. Changes in tidal asymmetry were characterized through the ratio between the amplitude of M4 and M2. The impact on sediment transport was characterized through the ratio between the sediments flushed at the inlet during the ebb and entering the lagoon during the flood. Results show that higher water levels reduce tidal asymmetry (figure 8-B), strongly decrease ebb-dominance, and the ratio between ebb and flood sand transport across the inlet tends to 1 (figure 8-C).



323
 324
 325 Figure 8. (A) Bathymetry of the Óbidos lagoon with the cross-section where sand transport was integrated, (B)
 326 ratio between the amplitudes of M4 and M2 in the lagoon and (C) residual sand transport across the inlet
 327 (ebb/flood).
 328 Figura 8. (A) Batimetria da Lagoa de Óbidos mostrando a secção transversal onde o transporte de areia foi
 329 integrado, (B) quociente entre as amplitudes da M2 e da M4 na laguna e (C) transporte de areia residual através
 330 da embocadura (vazante/enchente).

331
 332 Because floods occur, on average, at higher water levels than ebbs (Fortunato and Oliveira, 2007), the
 333 water flows more freely into, than out of, the lagoon. Floods are therefore shorter than ebbs, which would
 334 contribute to higher velocities on flood than on ebb. However, mass conservation also implies that the higher
 335 water depths on flood reduce the flood velocities relative to the ebb currents. While the former process is usually
 336 the dominant one in large estuaries and inlets, we found the latter to dominate in our two shallow lagoons.
 337 Raising the mean sea level has therefore two opposite effects. On the one hand, the higher water depth in the
 338 inlet facilitates the water outflow, thereby reducing the ebb duration and the flood dominance. For instance, the
 339 mean water level in the lagoon explains 50 % of the difference between ebb and flood durations in the Albufeira
 340 lagoon (Fortunato et al., 2014), with longer floods corresponding to higher mean water levels. On the other hand,
 341 the relative differences between the water depths on ebb and flood decrease, which reduces the distinction
 342 between ebb and flood velocities due to continuity. This process is illustrated on Figure 8C. Since tidal
 343 asymmetry is dominated by the mass conservation effect in shallow lagoons, raising the mean water level
 344 reduces the predominance of ebb currents in these systems.

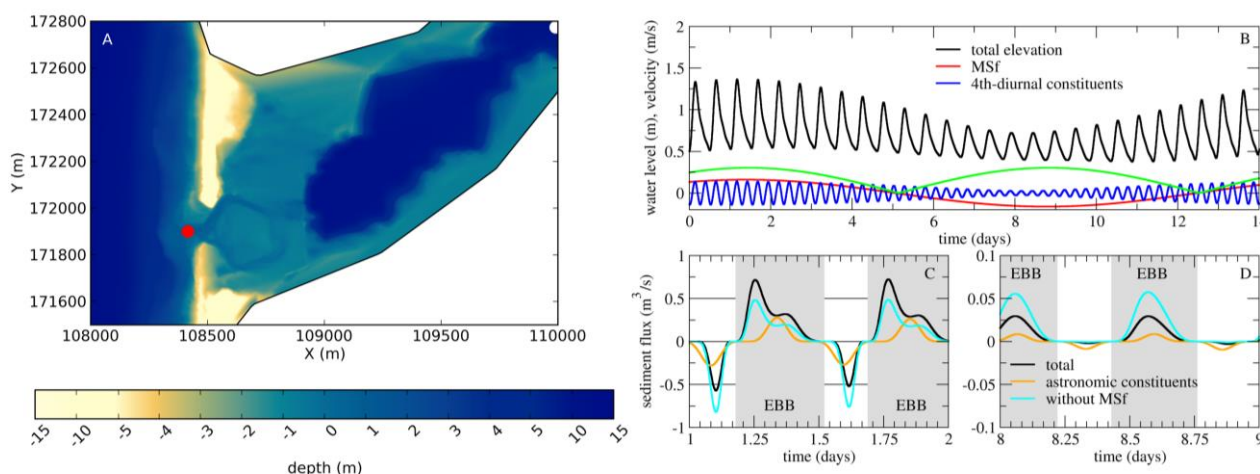
345 In addition to the wave-induced setup which develops in the nearshore, MSL experiences a seasonal
 346 cycle along the west coast of Portugal. A permanent tide gauge is located in the Cascais marina between both
 347 studied sites (figure 1). A Demerliac filter was applied to a time series of water level originating from this station
 348 and daily and monthly MSL were computed (figure 9). This figure reveals that mean sea-level reaches its
 349 maximum in autumn and its minimum in late winter, with a 0.2 m difference between both. Although outside the
 350 scope of this study, investigations in progress in our team show that this seasonal cycle results from the
 351 superimposition of atmospheric forcing and steric effects. The Albufeira Lagoon Inlet usually closes in autumn
 352 (e.g. Dodet et al., 2013): it is likely that the decrease in ebb-dominance related to a higher MSL can contribute
 353 significantly to inlet closure.
 354



355
 356 Figure 9. Daily and Monthly mean sea-level in Cascais between 2000 and 2007.

357 Figura 9. Médias diárias e mensais do nível do mar em Cascais entre 2000 e 2007.

358
359 Besides the rise in mean sea level associated to seasonal effects and storms, significant fortnightly
360 variations of water level can also occur inside the lagoon due to non-linear tides. These fortnightly
361 tides are particularly strong in very shallow systems. In the Albufeira lagoon, their amplitude reaches
362 several tens of centimetres, with crests occurring on spring tides and troughs on neap tides (Fortunato
363 et al., 2014). The importance of these constituents is shown at the Albufeira lagoon in a simulation
364 forced by M2 and S2 tidal constituents. The amplitude of the fortnightly constituent MSf reaches
365 about 15 cm. The associated velocity at the tidal inlet throat exceeds 30 cm/s. This velocity is in phase
366 with the elevations (Figure 10B), indicating that this constituent is a standing wave. These strong
367 velocities affect the sediment fluxes significantly. On spring tides they increase sediment fluxes on ebb
368 and decrease them on flood (Figure 10C). The opposite occurs on neap tides (Figure 10D). Hence, ebb
369 dominance from a sediment viewpoint is not only higher on spring tides due to the stronger fourth-
370 diurnal constituents, but also due to the fortnightly constituents.



371 Figure 10. (A) Bathymetry of the Albufeira lagoon inlet, relative to mean sea level. (B) Water levels
372 inside the lagoon obtained in a simulation forced by M2 and S2. MSf velocities at the inlet throat are
373 also shown as a dashed line. Sediment fluxes across the tidal inlet estimated with the Engelund and
374 Hansen (1967) formula on spring (C) and neap tides (D).

375
376 Figura 10. (A) Batimetria da embocadura da Lagoa de Albufeira, relativa ao nível médio do mar. (B)
377 Níveis dentro da laguna obtidos numa simulação forçada pelas constituintes M2 e S2. As velocidades
378 associadas à constituinte MSf no centro do canal da embocadura são mostradas a tracejado. Os fluxos
379 sedimentares através da embocadura foram calculados com a fórmula de Engelund e Hansen (1967)
380 em marés vivas (C) e mortas (D).

383 5. Conclusions and future works

384
385 This study presented a synthesis of the physical processes controlling the seasonal cycle of wave-
386 dominated inlets and revealed firstly that the inlet development during fair weather conditions was
387 caused by a huge tidal distortion that promotes ebb-dominance. The shoaling or closure of wave
388 dominated inlets during winter storm was explained by the superimposition of several wave-related
389 processes: (1) the “bulldozer effect” due to the shore-normal component of wave forces acting over the
390 ebb shoals; (2) the presence of lateral barotropic pressure gradients, accelerating longshore flows
391 towards the inlet; (3) wave blocking during the ebb; (4) the reduction of ebb dominance by a high
392 mean sea level in autumn and during storms; and (5) the presence of infragravity waves. In addition,

393 fortnightly overtides generated by non-linear processes enhance ebb-dominance on spring tides and
394 have the opposite effect on neap tides. This effect helps explaining the stronger tendency for inlet
395 closure on neap tides. While the impact of processes (1), (2) and (4) on inlet morphodynamics were
396 already quantified at the Óbidos Lagoon Inlet, the contribution of wave blocking and infragravity
397 waves remains to be investigated. Also, this study mostly investigates cross-shore wave induced
398 processes while oblique waves can induce strong inlet migration. The subsequent lengthening of the
399 channel can alter tidal propagation and limit the ability of the inlet to flush sediments. It is expected
400 that the proper representation of all these processes in morphodynamic modelling systems will allow
401 simulating the closure of wave-dominated inlets.

402 However, hydrodynamic conditions display relatively modest variations along the West Coast of
403 Portugal so that the physical processes analysed in this study may be partly site-specific. Their
404 importance will have to be investigated at other wave-dominated inlets, such as in SW Australia, South
405 Africa, California and Central and Southern America.

406 Also, other processes not discussed herein can affect the morphodynamics of tidal inlets. For
407 instance, channel meandering increases the risk of inlet closure (Behrens et al., 2009, 2013), while
408 fresh water flows promote its opening (Shuttleworth et al., 2005). Also, the curvature of the channel
409 affects the inlet migration (Chaumillon et al., 2014). Overall, the morphodynamics of wave-dominated
410 inlets is a complex problem, and its controlling mechanisms remain only partly understood.

411
412

413 **Acknowledgements**

414

415 This work was part of a project funded by the Portuguese Foundation for Science and Technology
416 (FCT): 3D-MOWADI (PTDC/ECM/103801/2008). Researches in progress are part of the research
417 project ANR JC DYNAMO (agreement ANR-12-JS06-00008-01). The wave models (SWAN) and the
418 circulation models (ELCIRC/SELFE) were provided by Delft University of Technology and the Center
419 for Coastal Margin Observation and Prediction, respectively. Topographic and hydrodynamic data
420 were obtained, thanks to the combined efforts of many individuals from the Faculty of Science of the
421 University of Lisbon, the National Laboratory of Civil Engineering, the University of Algarve and the
422 Instituto Hidrográfico. The time series of sea surface elevation at Cascais were provided by the
423 Portuguese Geographic Institute.

424

425

426

427 **References**

428

429 Behrens, D.K., Bombardelli, F.A., Largier, J.L., Twohy, E. (2009). Characterization of time and
430 spatial scales of a migrating river mouth, *Geophysical Research Letters*, 36.

431

432 Behrens, D.K., Bombardelli, F.A., Largier, J.L., Twohy, E. (2013). Episodic closure of the tidal
433 inlet at the mouth of the Russian River – A small bar-built estuary in California, *Geomorphology*,
434 189: 66-80.

435

436 Bertin X., Oliveira A. and Fortunato A.B. (2009a). Simulating morphodynamics with unstructured
437 grids: description and validation of a modelling system for coastal applications. *Ocean modelling*, 28 :
438 75-873.

439

440 Bertin X., Fortunato, A.B. and Oliveira A. (2009b). A modeling-based analysis of processes driving
441 wave-dominated inlets. *Continental Shelf Research*, 29: 819-834.

442

443 Bertin, X., Fortunato, A.B. and Oliveira, A. (2009c). Morphodynamic Modeling of the Ancao Inlet,
444 South Portugal. *Journal of Coastal Research*, SI 56, 10-14.

445

446 Bertin, X., Bruneau, N., Breilh, J.F., Fortunato, A.B. and Karpytchev, M. (2012). Importance of wave
447 age and resonance in storm surges: the case Xynthia, Bay of Biscay. *Ocean Modelling*, 42 (4): 16-30.

448

449 Booij, N., Ris, R., Holthuijsen, L. (1999). A third-generation wave model for coastal regions. 1. Model
450 description and validation. *Journal of Geophysical Research*, 104 (7): 649–666.
451

452 Bruneau, N., Fortunato, A.B., Dodet, G., Freire, P., Oliveira, A. and Bertin, X. (2011). Future evolution
453 of a tidal inlet due to changes in wave climate, Sea level and lagoon morphology (Óbidos lagoon,
454 Portugal). *Continental Shelf Research*, 31: 1915-1930.
455

456 Chaumillon, E., F. Ozenne, X. Bertin, N. Long, F. Ganthuy (2014). Wave climate and inlet channel
457 meander bend control spit breaching and migration of a new inlet: La Coubre sand spit, France,
458 *Journal of Coastal Research*, SI66.
459

460 Dastgheib, A., Roelvink, J.A., Wang, Z.B. (2008). Long term process-based morphological modeling of
461 the Marsdiep Tidal Basin. *Marine Geology*, 256: 90-100.
462

463 Dodet, G., Bertin, X., and Taborda, R. (2010). Wave climate variability in the North-East Atlantic
464 Ocean over the last six decades. *Ocean Modelling*, 31: 120-131.
465

466 Dodet, G., Bertin, X., Bruneau, B., Fortunato, A.B., Nahon, A. and Roland, A. (2013). Wave-current
467 interactions at a wave-dominated inlet. *Journal of Geophysical Research-Oceans*, 118: 1-19.
468

469 Dodet, G., 2013. Morphodynamic modelling of a wave-dominated tidal inlet: the Albufeira Lagoon.
470 Unpublished PhD thesis of La Rochelle University, 181 p.
471

472 Engelund, F., Hansen, E. (1967). A monograph on sediment transport in aluvial streams, Teknisk
473 Forlag, Technical University of Danmark, Ostervolgade, 10, Copenhagen, Denmark.
474

475 Fortunato, A.B., Oliveira, A. (2004). A modeling system for tidally driven long-term morphodynamics.
476 *Journal of Hydraulic Research*, 42: 426-434.
477

478 Fortunato, A.B., Oliveira, A. (2007). Case study: promoting the stability of the Óbidos lagoon inlet.
479 *Journal of Hydraulic Engineering*, 133/7: 816-824.
480

481 Fortunato, A.B., A. Nahon, G. Dodet, A.R. Pires, M.C. Freitas, N. Bruneau, A. Azevedo, X. Bertin, P.
482 Benevides, C. Andrade, A. Oliveira (2014). Morphological evolution of an ephemeral tidal inlet from
483 opening to closure: the Albufeira inlet, Portugal, *Continental Shelf Research*, 73: 49-63.
484

485 Friedrichs, C.T., Aubrey, D.G. (1988). Non-linear tidal distortion in shallow well-mixed estuaries: a
486 synthesis. *Estuarine, Coastal and Shelf Science*, 27: 521-545.
487

488 Hagemann, B.P. (1969). Development of the western part of the Netherlands during the Holocene.
489 *Geologie en Mijnbouw*, 48: 373-388.
490

491 Oliveira, A., A.B. Fortunato and J.R.L. Rego (2006). Effect of morphological changes on the
492 hydrodynamics and flushing properties of the Óbidos lagoon (Portugal). *Continental Shelf Research*,
493 26: 917-942.
494

495 Ranasinghe, R., Pattiaratchi, C. and G. Masselink (1999). The seasonal closure of tidal inlets: Wilson
496 Inlet, a case study. *Coastal Engineering*, 37: 37-56.
497

498 Roelvink, J.A., Reniers, A., Van Dongeren, A., Van Thiel de Vries, J., McCall, R., Lescinski, J. (2009).
499 Modeling storm impacts on beaches, dunes and barrier islands. *Coastal Engineering*, 56:1133-1152.
500

501 Roland, A., Zhang, Y.J., Wang, H.V., Meng, Y., Teng, Y-C, Maderich, V., Brovchenko, I., Dutour-
502 Sikiric, M. and Zanke, U. (2012). A fully coupled 3D wave-current interaction model on unstructured
503 grids. *Journal of Geophysical Research*, 117, C00J33.
504

505 Shuttleworth, B., A. Woidt, T. Paparella, S. Herbig and D.J. walker (2005). The dynamic behaviour of
506 a river-dominated tidal inlet, tiver Murray, Australia, *Estuarine, Coastal and Shelf Science*, 64: 645-
507 657.
508 Soulsby, R., 1997. Dynamics of marine sands, a manual for practical applications. Thomas Telford,

509 ISBN 0-7277-2584X, H.R. Wallingford, England.

510

511 Tung, T.T., Walstra, D.J., Graaff, J. van de and Stive, M. (2009). Morphological modeling of tidal inlet
512 migration and closure. *Journal of Coastal Research*, SI 56 (Proceedings of the 10th International
513 Coastal Symposium), 1080 – 1084. Lisbon, Portugal, ISSN 0749-0258.

514

515 Westhuysen, A. (2012). Spectral modeling of wave dissipation on negative current gradients. *Coastal
516 Engineering*, 68: 17–30.

517

518 Zhang, Y., Witter, R.W., Priest, G.P. (2011). Nonlinear tsunami-tide interaction in 1964 Prince William
519 Sound tsunami. *Ocean Modelling*, 40 (3–4), 246–259

520

521